4ICEGE Thessaloniki-GREECE 2007

4th International Conference on
Earthquake Geotechnical Engineering
June 25-28, 2007
Paper No. 1326

APPROXIMATE EVALUATION OF NONLINEAR EFFECTS ON SEISMICALLY INDUCED IN-PLANE STRESSES IN TUNNEL LININGS

Hany EL NAGGAR [1], Sean HINCHBERGER[2] and M. Hesham EL NAGGAR[3]

ABSTRACT

Seismic effects should be considered during the design of tunnel linings in active seismic regions. In addition, closed-form solutions are often useful for preliminary design of tunnels since they permit economic and efficient evaluation of design options without the need for complicated or more sophisticated methods of analysis. In this paper, a closed-form solution for composite tunnel linings in a homogeneous infinite isotropic elastic medium is modified to account for the in-plane shear stresses induced by earthquakes. The solution treats the tunnel lining as an inner thin-walled shell coupled with an outer thick-walled cylinder embedded in linear elastic soil or intact rock. The effect of in-plane shear stress is considered by assuming that the free-field ground response produced during an earthquake is perpendicular to the tunnel's longitudinal axis. In addition, the effect of local soil nonlinearity caused by earthquakes around bored tunnels is investigated using the equivalent linear approach. The non-linearity is accounted for by introducing an annular zone of soil around the tunnel with a degraded shear modulus. The shear modulus of such a degraded or weakened zone (modeled as a thick-walled cylinder) can be estimated based on the strain level within the soil adjacent to the tunnel. Solutions for moment and thrust have been derived for cases involving slip and no slip at the liner-ground interface. A parametric study was performed to investigate the effect of soil nonlinearity on the seismically induced moments and thrusts in a tunnel lining.

Keywords**:** analytical solution, tunnel lining, in-plane shear, weakened zone, internal forces

INTRODUCTION

The population density in urban centres necessitates construction of new underground transportation systems to address social and economical needs. The design and construction of tunnels poses several technical challenges, of which predicting the internal forces in tunnel linings for different loading cases is one of the major challenges.

Seismic effects on buried structures represent a major design consideration in active seismic regions. Hindy and Novak (1979; 1980) studied the axial deformation of pipelines induced by seismic waves propagating in the longitudinal direction of the pipelines. Atkinson et al. (1982) studied the in-plane bending moments induced by spatial incoherence of seismic waves. Merrit et al. (1985) and Wang (1993) studied various aspects of the global seismic response of tunnels using the solution presented by Peck et al. (1972), which assumes a hydrostatic stress field around the tunnel (Ko=1.0). Penzien and Wu (1998) and Penzien (2000) considered the effect of in-plane shear stress on tunnel linings induced by earthquakes assuming that the free-field ground response is perpendicular to the tunnel's

[1] Research Assistant, Department of Civil & Environmental Engineering, The University of Ontario, Canada, Email: helnagg2@uwo.ca
[2] Assistant Professor, Department of Civil & Environmental Engineering, The University of Ontario, Canada, Email: Shinchbe@uwo.ca
[3] Professor, Department of Civil & Environmental Engineering, The University of Ontario, Canada, Email: helnaggar@eng.uwo.ca

longitudinal axis. However, none of these studies have considered the effect of a weakened or degraded zone that can form around bored tunnels due to the construction process or to seismically induced shear waves.

In this paper, a closed-form solution for composite tunnel linings in a homogeneous infinite isotropic elastic medium is utilized to account for the in-plane shear stress induced by earthquakes. Solutions for moment and thrust have been derived for cases of slip and no slip at the lining-ground interface. In addition, the effect of nonlinearity of a weakened or degraded zone around the tunnel is investigated using the equivalent linear approach.

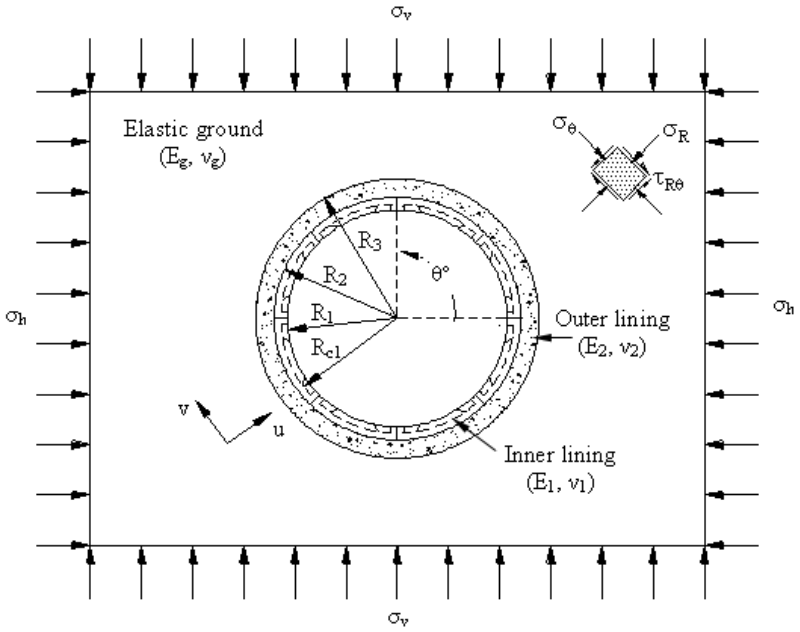

Figure 1. Problem geometry – double liners system.

THE DOUBLE LINER SOLUTION

El Naggar et al. (2006) developed an analytical solution to calculate the internal forces in composite circular tunnel linings embedded in a homogenous infinite elastic medium and subjected to an initial anisotropic stress field as shown in Figure 1. The initial vertical and horizontal stresses in the ground are σ_v and σ_h, respectively, where $\sigma_h = K_o \sigma_v$ and K_o is the coefficient of lateral earth pressure. For the solution, the initial stress field (see Fig 2) is separated into a hydrostatic component, $P_o = (\sigma_v + \sigma_h)/2$ and a deviatoric component, $Q_o = (\sigma_h - \sigma_v)/2$. The moment and thrust are determined in terms of the angle, θ measured counter clockwise with respect to the spring line axis of the tunnel.

The closed-form solution (El Naggar et al. 2006) assumes that the lining comprises an inner thin-walled shell with elastic modulus E_1, Poisson's ratio ν_1, cross-sectional area A_1, and moment of inertia, I_1. The intrados and extrados of the inner lining are defined by R_1 and R_2, respectively. The inner lining is surrounded by a thick annulus of soil (or a secondary liner as in the original solution) that is modeled as a thick-walled cylinder with elastic modulus E_2, Poisson's ratio ν_2 and inner and outer radii R_2 and R_3, respectively. The thin-walled shell and thick-walled cylinder are embedded in elastic ground (e.g. strong soil or intact rock) with elastic modulus E_g and Poisson's ratio ν_g. Plane strain conditions are assumed.

In order to derive the solution, it is assumed that tunnel construction relieves the *in situ* stresses in the ground, hence reducing the boundary stresses around the circumference of the tunnel at $r = R_3$ until new boundary stresses are reached that are in equilibrium with the liner reactions. This condition is imposed to derive the solutions for moments and thrust in the composite tunnel lining for the case of

no slip at $r = R_2$ and $r = R_3$. The solutions for cases of slip and no slip at $r = R_2$ and $r = R_3$, and full slip at both $r = R_2$ and $r = R_3$ are presented in El Naggar et al. (2006).

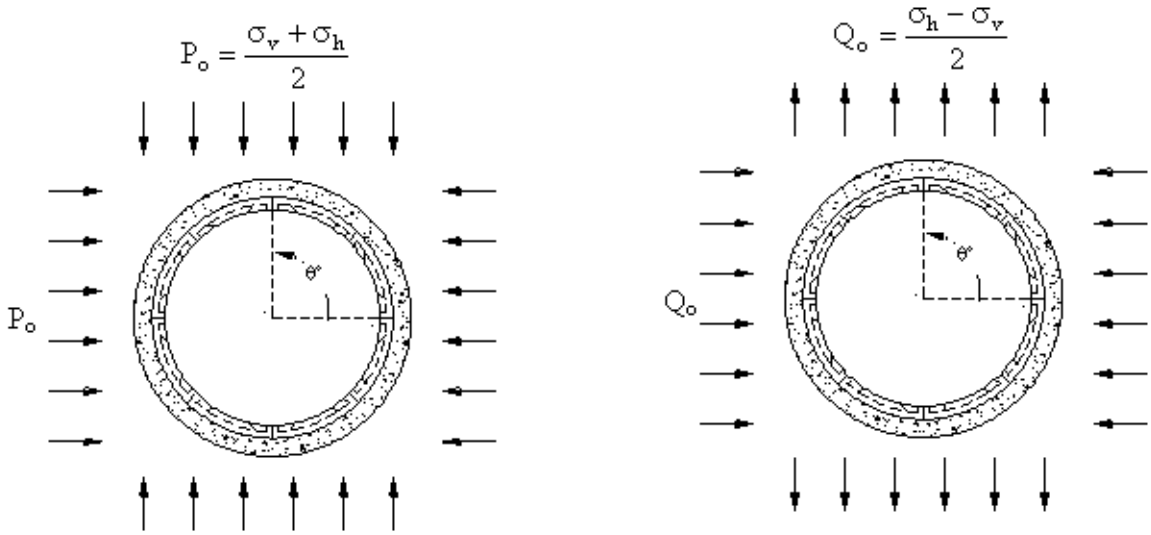

Figure 2. Hydrostatic and deviatoric components of the solution.

LINER REACTIONS AND INTERNAL FORCES DUE TO TUNNELLING

Using Airy's stress function, solutions were developed for the ground response due to full stress relief (e.g. Timoshenko and Goodier 1934; Jaeger and Cook 1976) at $r = R_3$ and for the reactive forces at $r = R_3$ caused by the presence of the liner (e.g. Morgan 1961; Muir Wood 1975; and Yuen 1979). In this paper, Airy stress function was used in conjugation with the thick-walled cylinder equations (Timoshenko and Goodier 1934), and the thin-walled shell equations (Flügge 1966) to solve for the liner's reactions and internal forces.

Hydrostatic Component

For the hydrostatic component (see Fig. 3a), the outer and inner liner reactions at $r = R_3$ and $r = R_2$ are in the radial direction and denoted by σ_{N2}^H and σ_{N1}^H, respectively. The displacement continuity condition in the radial direction is satisfied as follows: at the ground-outer lining interface by equating the displacement of the outer lining to the total ground displacement and by superposition of solutions for full stress relief and the reactive force, σ_{N2}^H; and at the interface between the outer lining and the inner lining (at $r = R_2$) by equating the radial displacement of the inner and outer linings. Thus, the explicit solution for σ_{N2}^H and σ_{N1}^H are (El Naggar et al. 2006):

$$\sigma_{N1}^H = \frac{(1-\Omega)\,P_o}{C_1\,(C_2 + C_3 C_7) + C_7} \qquad [1]$$

$$\sigma_{N2}^H = \frac{(1-\Omega)\,P_o C_7}{C_1\,(C_2 + C_3 C_7) + C_7} \qquad [2]$$

where the coefficients C_1 through C_7 inclusive are:

$$C_1 = \frac{E_g\,(1+\nu_2)}{E_2\,(1+\nu_g)},\ C_2 = -\frac{2\,(1-\nu_2)h}{(1-h)},\ C_3 = \frac{h + (1-2\nu_2)}{(1-h)},\ C_4 = \frac{R_{c1}^4}{D_{c1}\,R_{c1}^2 + D_{f1}},$$

$$C_5 = \frac{(1+\nu_2)}{E_2(1-h)}(-1-(1-2\nu_2)h)\,R_2,\ C_6 = \frac{2\,(1+\nu_2)(1-\nu_2)}{E_2\,(1-h)}\,R_2 \text{ and } C_7 = \frac{(C_4 - C_5)}{C_6}$$

and $h = (R_2 / R_3)^2$, $D_{c1} = E_1 A_1 / (1 - \nu_1^2)$ and $D_{f1} = E_1 I_1 / (1 - \nu_1^2)$.

From the reactions σ_{N2}^H and σ_{N1}^H at $r = R_3$ and $r = R_2$, the moment and thrust are:

$$M^H = - \frac{D_{f1} R_{c1}^2}{D_{c1} R_{c1}^2 + D_{f1}} \sigma_{N1}^H \quad [3]$$

$$T^H = \frac{D_{c1} R_{c1}^3}{D_{c1} R_{c1}^2 + D_{f1}} \sigma_{N1}^H + \frac{M^H}{R_{c1}} \quad [4]$$

a)

b)

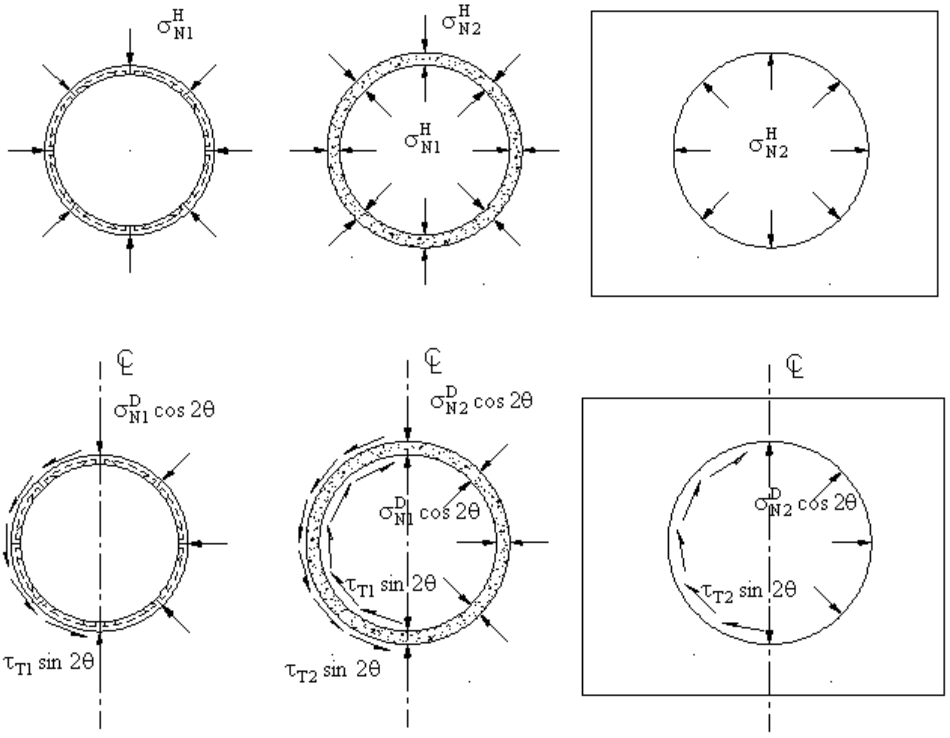

Figure 3. Reactive stresses – a) Hydrostatic component, b) Deviatoric component.

Deviatoric Component

For the deviatoric component (see Fig. 3b), the liner reactions in the radial and tangential directions at $r = R_3$ are denoted by $\sigma_{N2}^D \cos 2\theta$ and $\tau_{T2} \sin 2\theta$, and at $r = R_2$ by $\sigma_{N1}^D \cos 2\theta$ and $\tau_{T1} \sin 2\theta$. Similar to the hydrostatic component case, the continuity condition in the radial direction is satisfied by equating the displacement of the outer lining at $r = R_3$ to the total ground displacement caused by full stress relief and the reactive force, σ_{N2}^D. In addition, the reactions of the outer and inner liners at $r = R_2$ must be in equilibrium and the displacements are equal. The continuity in the tangential direction, on the other hand, is dependent on the assumed slippage conditions (i.e. no slip or full slip). For example, the conditions for no slippage at both interfaces (at $r = R_2$ and $r = R_3$) are: equal tangential displacement of the outer liner and the ground at $r = R_3$, and equal tangential displacement for both liners at their interface ($r = R_2$). For the case of full slip at both interfaces, the tangential displacements of the outer and inner liners are independent and not equal. The explicit solutions for the radial and tangential reactive forces are presented in the following section for the case of no slip at both interfaces. For other cases refer to El Naggar et al. (2006).

Case of No Slip at $r = R_2$ and $r = R_3$

For the case of no slip at both $r = R_2$ and $r = R_3$, the boundary conditions are: $\sigma_R = \sigma_{N2}^D \cos 2\theta$ and $\tau_{R\theta} = \tau_{T2} \sin 2\theta$ at $r = R_3$, $\sigma_R = \sigma_{N1}^D \cos 2\theta$ and $\tau_{R\theta} = \tau_{T1} \sin 2\theta$ at $r = R_2$ and $\sigma_R = \tau_{R\theta} = 0$ at $r = \infty$. Thus, the explicit solutions for the reactive forces are given by (El Naggar et al. 2006):

$$\sigma_{N2}^D = \frac{3(1-\Omega)Q_o(3-4\nu_g)(\frac{a_{13}}{\Lambda} + a_{14})}{(a_{31} + a_{32}\Gamma)(\frac{a_{13}}{\Lambda} + a_{14}) - (a_{11} + a_{12}\Gamma)(\frac{a_{33}}{\Lambda} + a_{34})} \quad [5]$$

$$\sigma_{N1}^D = \Gamma \sigma_{N2}^D \quad [6]$$

$$\tau_{T2} = -\frac{3(1-\Omega)Q_o(3-4\nu_g)(a_{11} + a_{12}\Gamma)}{(a_{31} + a_{32}\Gamma)(a_{13} + a_{14}\Lambda) - (a_{11} + a_{12}\Gamma)(a_{33} + a_{34}\Lambda)} \quad [7]$$

$$\tau_{T1} = \Lambda \tau_{T2} \quad [8]$$

where,

$$\Gamma = -\frac{(a_{31} - a_{41})(a_{14}a_{23} - a_{24}a_{13}) + (a_{33} - a_{43})(a_{11}a_{24} - a_{21}a_{14}) + (a_{34} - a_{44})(a_{21}a_{13} - a_{11}a_{23})}{(a_{32} - a_{42})(a_{14}a_{23} - a_{24}a_{13}) + (a_{33} - a_{43})(a_{12}a_{24} - a_{22}a_{14}) + (a_{34} - a_{44})(a_{22}a_{13} - a_{12}a_{23})} \quad [9]$$

$$\Lambda = -\frac{(a_{31} - a_{41})(a_{22}a_{13} - a_{12}a_{23}) + (a_{32} - a_{42})(a_{11}a_{23} - a_{21}a_{13}) + (a_{33} - a_{43})(a_{21}a_{12} - a_{11}a_{22})}{(a_{31} - a_{41})(a_{22}a_{14} - a_{12}a_{24}) + (a_{32} - a_{42})(a_{11}a_{24} - a_{21}a_{14}) + (a_{34} - a_{44})(a_{21}a_{12} - a_{11}a_{22})} \quad [10]$$

and the coefficients a_{11} to a_{44} and α_1 to ω_1 are summarized in the appendix.

Thus, the moments and thrusts in the inner lining due to the deviatoric component are:

$$M^D = -\frac{D_{f1}}{R_{c1}^2}\left[-3C_8\left(\alpha_1\sigma_{N2}^D + \beta_1\tau_{T2} + \chi_1\sigma_{N1}^D + \delta_1\tau_{T1}\right)\right]\cos 2\theta \quad [11]$$

$$T^D = \left[\frac{D_{c1}}{R_{c1}} C_8\left[(\alpha_1 + 2\psi_1)\sigma_{N2}^D + (\beta_1 + 2\gamma_1)\tau_{T2} + (\chi_1 + 2\eta_1)\sigma_{N1}^D + (\delta_1 + 2\omega_1)\tau_{T1}\right] + \frac{M^D}{R_{c1}}\right]\cos 2\theta \quad [12]$$

(Note: $C_8 = (1+\nu_2)R_2/(3E_2(1-h)^3)$)

The In-Plane Shear Wave Component

Distortion of the cross-section (ovaling) of a tunnel's liner during an earthquake can severely compromise its integrity (Wang, 1993 and Hashash et al., 2001). Ovaling or racking deformation in a tunnel is developed due to the in-plane shear stresses caused by the vertically propagating horizontal shear waves induced by an earthquake. Generally, there are two basic approaches in present seismic design practices. In the first approach, a full dynamic non-linear soil-structure interaction analysis is performed using for example the finite element method. In this approach, the time history of the motion is applied to represent the vertically propagating shear waves. In the second approach, the pseudo-static approach, the earthquake loading is simulated by applying a static far-field shear stress or shear strain at the model boundaries to represent the seismic effects.

Current seismic design approaches for circular tunnels suggest the use of the pseudo-static approach (e.g. Hendron and Fernandez, 1983; Merritt et al., 1985; Penzien and Wu, 1998; and Penzien, 2000). In this approach, the in-plane shear stress is assumed to be linear over the tunnel's diameter. Using the vertically propagating shear wave model, the average free-field shear strain of the soil in the transverse plane, γ_c, can be obtained from ground response analyses. Thus, the corresponding state of stress is of the shear type shown in Figure 4a, which is equivalent to the state of stress considered by Penzien, 1998, shown in Figure 4b. The magnitude of the far-field shear stress, τ_{ff}, is then equal to:

$$\tau_{ff} = \gamma_c G \qquad [13]$$

where γ_c is the shear strain, and G is the shear modulus of the soil.

As shown in Figure 4b, the earthquake loading component imposes loading conditions similar to that of the deviatoric component. Consequently, the moment and thrust due to the earthquake component can be derived from the solution for the deviatoric component by substituting into Equations 5 through 12, inclusive, the value of τ_{ff} for Q_o and replacing θ with $(\theta + 3\pi/4 - \lambda)$, where λ is the angle with horizontal at which the earthquake waves will travel in the vertical plane as shown in Figure 5. For far-field earthquakes as shown in Figures 4a and 4b, λ is normally taken to be $\pi/2$ or 90°(e.g. Wang 1993; Penzien and Wu 1998 and Penzien 2000).

Finally, to obtain the overall stresses in the tunnel liner, the seismic induced stresses are superimposed on the initial stresses (e.g., after construction).

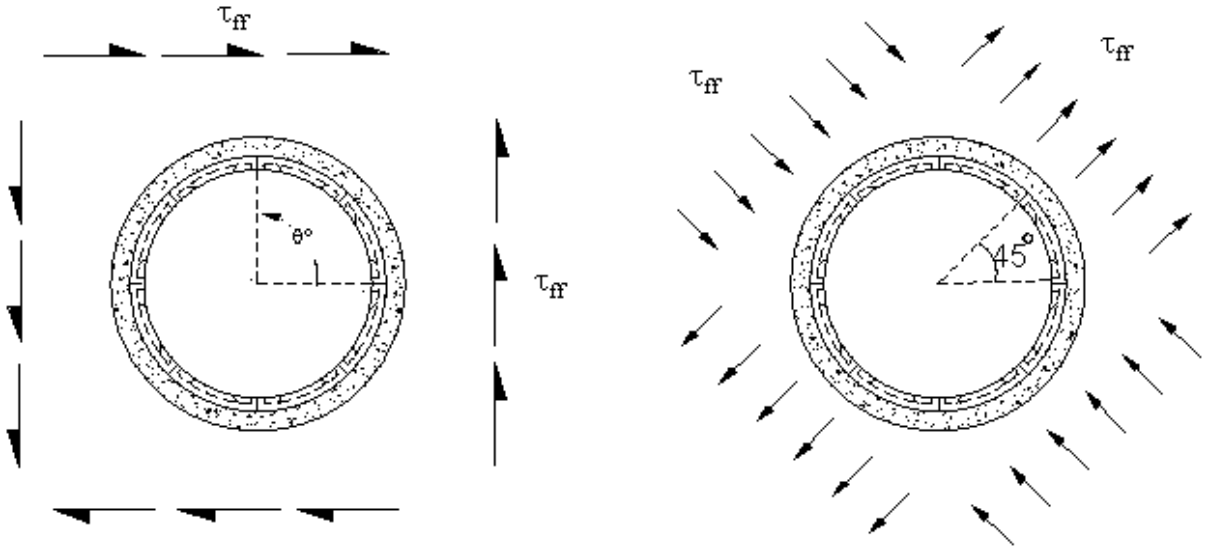

Figure 4. a) Earthquake induced shear stresses, b) Equivalent principle stresses

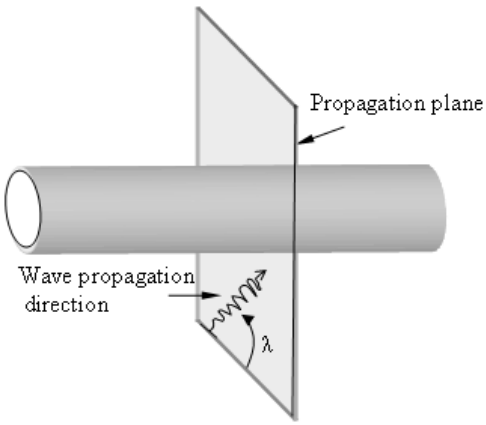

Figure 5. The incidence angle

APPLICATION OF THE THEORY

In this section, the seismic performance of a typical subway tunnel in a seismic active region is investigated using the approach summarized above. The effect of nonlinearity of soil adjacent to the tunnel is accounted for using the outer thick-walled cylinder in order to simulate a weakened or degraded annular zone. It is assumed that the tunnel passes through a homogeneous soil medium and that the groundwater table is far below the tunnel elevation.

The tunnel lining considered comprises 8 precast concrete segments and a key segment situated at the crown: each segment is 600mm wide. The segments are bolted together in the tangential direction to form rings and the rings are bolted together in the longitudinal direction to form the tunnel lining. The nominal liner thickness is 150mm, the inside diameter is 4.88m and the outside diameter (O.D.) is 5.18m. Table 1 summarizes the average soil parameters and the geometric properties of the tunnel that were used in the analysis. The effect of joints on the bending rigidity of the lining has been neglected.

Table 1: Material Parameters used in the analysis

Parameter	Value	Parameter	Value
Soil elastic modulus, E_g (MPa)	90	Elastic modulus of concrete, E_1 (GPa)	30
Soil Poisson's ratio, ν_g	0.4	Poisson's ratio of concrete, ν_1	0.2
Coeff. of earth pressure at rest, K_o'	0.7	Initial vertical stress, σ_v (kN/m^2)	344
Earthquake induced shear strain, γ_c	0.0028	Initial horizontal stress, σ_h (kN/m^2)	241

Effect of the Weakened Zone

In general, it is possible to have an annular zone adjacent to the tunnel that has been disturbed due to the construction process (i.e. excavation damage zone (EDZ), Tsang et al., 2004) or due to earthquake-induced high strains. Thus, an extensive parametric study was conducted to investigate the effect of this disturbed zone on the internal forces of the tunnel liner. The weakened zone was modeled as an outer thick-walled cylinder with ratios of its shear modulus to that of the ground, G_2/G_g, ranging from 0.1 to 1. The thickness of the weakened zone, t_w, to the centerline radius of the tunnel, R_{c1}, ranged from t_w/R_{c1}= 0.05 to 0.2.

Figures 6a to 6d summarize the results of the analysis which includes the initial liner loads and the seismically induced loads. Figures 6a and 6b show the moments at crown and at $\theta = 45^o$ locations. It can be seen that as G_2/G_g decreases (i.e. increased nonlinearity or disturbance) the moments increase. Figures 6a and b also show that the moments increase with an increase in the size of the disturbed

zone. This trend is expected because as the shear modulus of the disturbed zone decreases, the liner becomes more rigid relative to the disturbed zone, thus, attracting more load.

The thrust at the crown and at $\theta = 45^{o}$ is shown in Figures 6c and 6d. It is noted from the figures that the effect of nonlinearity is only significant for G_2/G_g below 0.4, at which point the thrust starts to decrease rapidly. The effect of the size of the disturbed zone on thrust is opposite to that observed for moments. The thrust decreases with an increase in the size of the disturbed zone. Generally, it can be concluded that as G_2/G_g decreases (higher nonlinearity) the moments increase and the thrust decreases causing tensile stresses to develop in the lining as discussed later on.

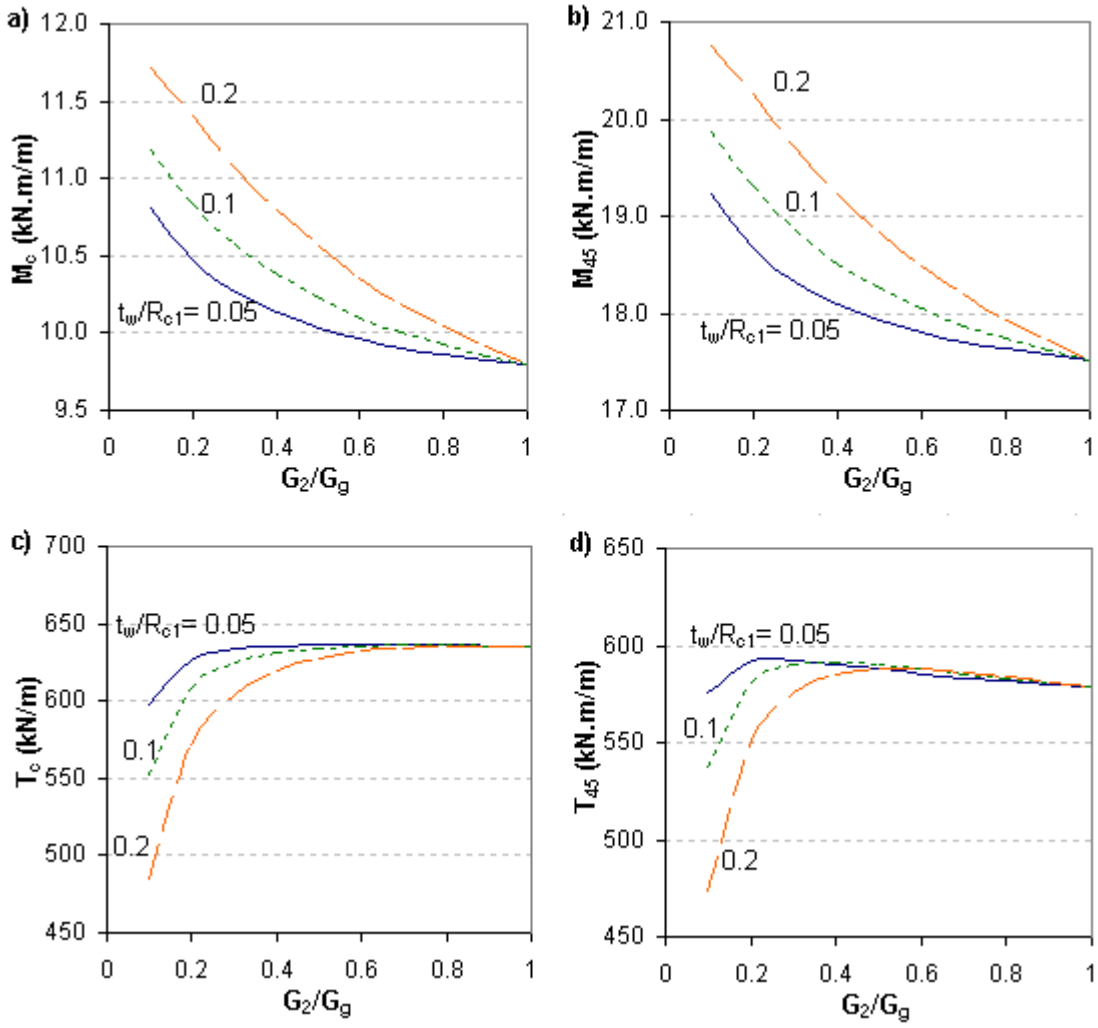

Figure 6. The effect of the nonlinearity of the weakened zone on the internal forces of the liner

Effect of the Angle of Incidence

The incident angle, λ, is the angle with horizontal at which the earthquake waves will travel in the vertical plane (plane perpendicular to the tunnel's longitudinal axis) as shown in Figure 5. Wang (1993), Penzien and Wu (1998) and Penzien (2000) suggested that this angle is 90°, i.e., vertically propagating seismic waves. The consideration of vertically propagating shear waves constitutes a simplification of the actual phenomenon, especially in the case of near-field events involving complex wave fields. For example, in the case of the 2003 Bam earthquake, Iran, the focal region of the main event was at a horizontal distance of about 3 km and at a depth of about 8-10km. By applying Snell's law and utilizing the shear wave velocities of soil strata in the region, it can be shown that at least a

significant portion of the seismic waves arrived at some angle with the vertical direction, i.e., the incident angle of the earthquake waves was not 90° (Rayhani and El Naggar, 2004).

The incident angle, λ, will affect the moments and thrusts resulting from seismically induced in-plane shear stresses whereas λ does not affect the initial stresses in the lining prior to an earthquake. Thus, to investigate the impact of λ, Figures 7a through d show only the internal forces in the tunnel lining due to seismically induces shear stresses for incident angles, λ, other than 90° (i.e. racking is not in the horizontal direction, see Fig. 5).

Referring to Figures 7a through d, it can be seen that the moment and the tensile thrust at the crown increase as the incident angle increases until it reaches a maximum at $\lambda = 45^{o}$ after which it decreases again to zero at $\lambda = 90^{o}$ (due to the rotation of the principle stresses as λ varies). Accordingly, the highest tensile stress at the crown at the inner face occur when earthquake waves impact the tunnel at $\lambda = 45^{o}$. The moment at the 45° location changes from positive (tension at the inner face) for $\lambda < 45°$ to negative (compression at the inner face) at incident angles greater than 45°. The maximum moment at the 45° location occurs at incident angles 0° and 90°. Figures 7c and d show that the variation of the thrust with the angle of incidence follows a similar trend to that observed for the moments.

Discussion of Results

The moments and thrust at the crown in the liner due to the *in situ* stresses (the post construction stresses) without considering the nonlinearity of the weakened zone are 9.8 kNm/m and 640 kN/m, respectively. The moment and thrust at the 45° location are zero and 540 kN/m. Thus, for an un-jointed liner, the critical design section is the crown with M_c=9.8 kN.m/m and T_c=640 kN/m and the maximum stress at the inner face of the critical section is 1.65 MPa (compression).

Referring to Figure 6, if seismic effects are considered with a weakened or degraded zone around the tunnel, then the moments at the crown may increase by up to 20% and the thrust may decrease by up to 23% (see results for G_2/G_g=0.1 and t_w/R_{c1}=0.2) and the resultant stress at the inner face of the critical section decreases to about zero (e.g. tensile stresses will start to develop).

By taking into account the earthquake component (with $\lambda = 90^{o}$), the critical design section becomes the 45° location with a moment of 20.8 kN.m/m and a thrust of T_c=430 kN/m, which represents an increase of the design moment of approximately 110% and a decrease in thrust in the range of 33%. Accordingly, for this case a tensile stress of 2.68 MPa develops at the inner face of the critical section, which is close to the tensile strength of the concrete.

The angle of incidence, λ, plays an important role in the selection of the critical section for continuous un-jointed linings. For example, if $\lambda = 0°$ or $90°$ the critical section will be at the 45° location, whereas, if $\lambda = 45°$ the critical section will be at the crown as can be seen from Figure 7. Thus for $\lambda = 45°$, the critical design section will be at the crown where M_c=30.3 kN.m/m and T_c=615 kN/m. Consequently, for $\lambda = 45°$ the maximum tensile stress at the inner face of the critical section is 3.98 MPa, which is close to the tensile strength of the concrete and may result in significant structural cracks in un-reinforced concrete linings or in linings without adequate reinforcement.

SUMMARY AND CONCLUSIONS

In this paper, a closed-form solution for moments and thrusts in a composite tunnel lining was utilized to account for the in-plane shear stresses induced by vertically propagating earthquake waves. In the solution, the ground is treated as an infinite elastic medium subject to an initial anisotropic stress field. The tunnel lining is idealized as an inner thin-walled shell surrounded by an annulus of weakened or degraded soil (an outer thick-walled cylinder).

In general, the solution was shown to be useful for preliminary design purposes since it permits economic and efficient evaluation of design options without the need for complicated or more sophisticated methods of analysis. This solution is suitable for the analysis of circular tunnels installed in either intact rock or strong soils above the groundwater table and that remain predominantly elastic during construction of the tunnel.

The effect of the soil nonlinearity caused by earthquakes around bored tunnels was investigated using the equivalent linear approach. In order to account for the soil nonlinearity approximately, a weakened annular zone of soil was considered around the tunnel. The results of the analysis showed that as the nonlinearity and/or the size (extent) of the weakened zone increases, the moments increase and the thrust decreases, causing under some circumstances tensile stresses to be induced in the liner.

The effect of the incidence angle, λ , on moments and thrust of the liner was investigated. It was found that the highest tensile stresses at the crown at the inner face occur when earthquake waves hits the tunnel at 45° with the horizontal axis. At this incidence angle, the moment at the crown of un-jointed liners may increase by up to 200%.

Finally, based on the analysis and discussion presented in this paper, it is concluded that the effect of the nonlinearity of the weakened or degraded zone and the in-plane shear stress induced by earthquakes is significant and should be considered in the design process.

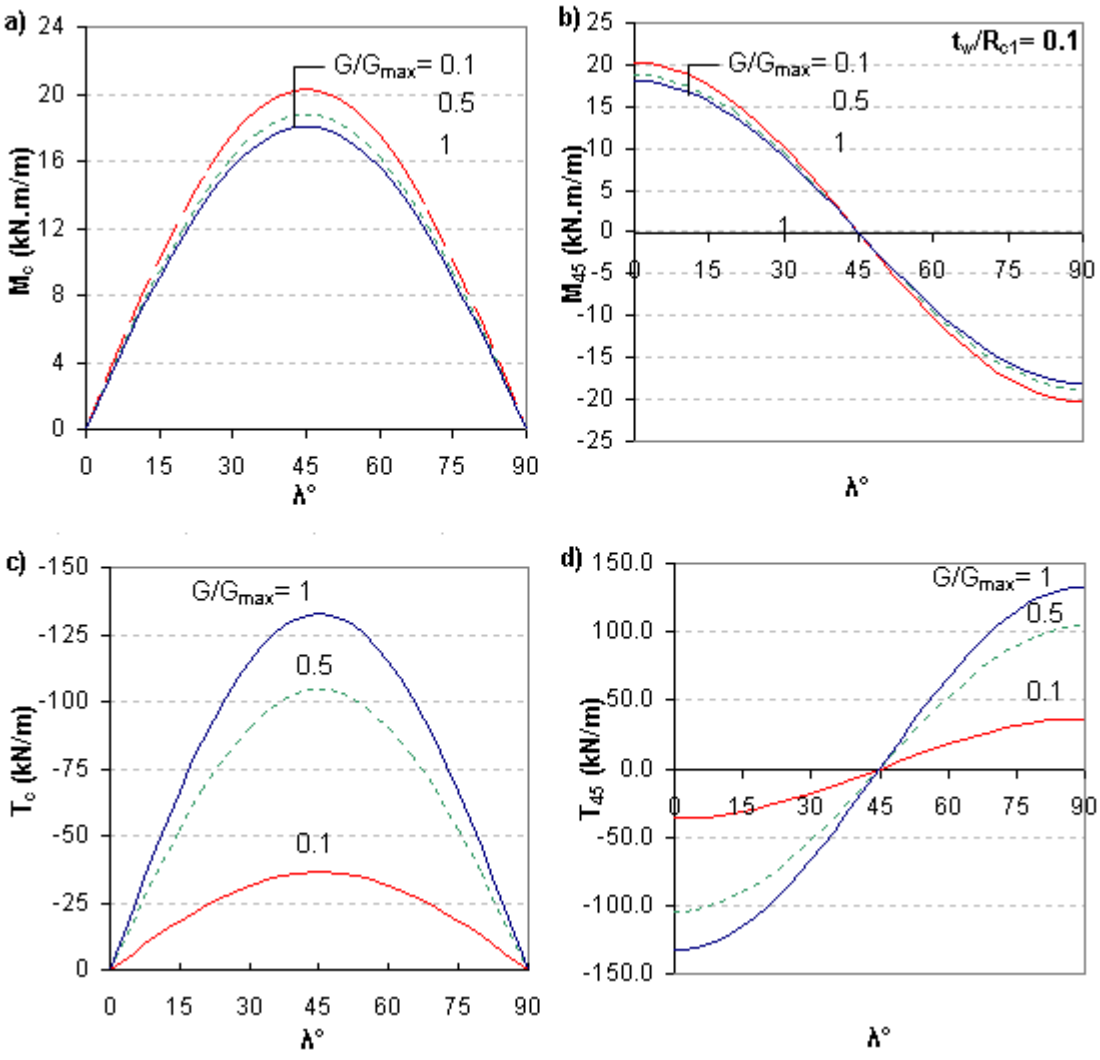

Figure 7. The effect of the angle of incidence on the internal forces of the liner

APPENDIX

$\alpha_1 = -\chi_2 / h$, $\beta_1 = \eta_2 / h$, $\chi_1 = -(3-2\nu_2)h^3 - (15-18\nu_2)h^2 - (9-6\nu_2)h - (5-6\nu_2)$

$\delta_1 = -2\nu_2 h^3 + 6\nu_2 h^2 - (12-6\nu_2)h - (4-6\nu_2)$, $\psi_1 = \delta_2 / h$, $\gamma_1 = -\omega_2 / h$

$\eta_1 = -\delta_1$, $\omega_1 = (3-2\nu_2)h^3 - (9-6\nu_2)h^2 + (9-6\nu_2)h + (5-6\nu_2)$,

$\alpha_2 = (5-6\nu_2)h^3 + (9-6\nu_2)h^2 + (15-18\nu_2)h + (3-2\nu_2)$

$\beta_2 = (4-6\nu_2)h^3 + (12-6\nu_2)h^2 - 6\nu_2 h + 2\nu_2$, $\chi_2 = -4(1-\nu_2)h(3h^2 + 2h + 3)$

$\delta_2 = -4(1-\nu_2)h(h+3)$, $\psi_2 = -\beta_2$, $\gamma_2 = -(5-6\nu_2)h^3 - (9-6\nu_2)h^2 + (9-6\nu_2)h - (3-2\nu_2)$

$\eta_2 = 4(1-\nu_2)h^2(3h+1)$, $\omega_2 = 8(1-\nu_2)h^2$

and

$$a_{11} = -4C_8\psi_1 - 2C_8\alpha_1 \qquad a_{21} = 2C_8\psi_1 + C_8\alpha_1 + \frac{9D_{F_1}}{D_{C_1}R_{c1}^2}C_8\alpha_1 \qquad a_{31} = C_{10} + C_9\alpha_2$$

$$a_{12} = -4C_8\eta_1 - 2C_8\chi_1 \qquad a_{22} = 2C_8\eta_1 + C_8\chi_1 + \frac{9D_{F_1}}{D_{C1}R_{c1}^2}C_8\chi_1 - \frac{R_{c1}^2}{D_{C_1}} \qquad a_{32} = C_9\chi_2$$

$$a_{13} = -4C_8\gamma_1 - 2C_8\beta_1 \qquad a_{23} = 2C_8\gamma_1 + C_8\beta_1 + \frac{9D_{F1}}{D_{C1}R_{c1}^2}C_8\beta_1 \qquad a_{33} = C_{11} + C_9\beta_2$$

$$a_{14} = -4C_8\omega_1 - 2C_8\delta_1 - \frac{R_{c1}^2}{D_{C1}} \qquad a_{24} = 2C_8\omega_1 + C_8\delta_1 + \frac{9D_{F_1}}{D_{C_1}R_{c1}^2}C_8\delta_1 \qquad a_{34} = C_9\delta_2$$

$$a_{41} = C_{11} - C_9\psi_2 \qquad a_{42} = -C_9\eta_2 \qquad a_{43} = C_{10} - C_9\gamma_2$$

$$a_{44} = -C_9\omega_2$$

REFERENCES

Atkinson, G. M., Davenport, A. G. and Novak, M. 1982. “Seismic risk to pipelines with application to Northern Canada,” Canadian Journal of Civil Engineering, Vol. 9, pp. 248-264.

El Naggar, H., Hinchberger, S. and Lo, K. Y. 2006. “A closed-form solution for tunnel linings in a homogenous infinite isotropic elastic medium”, Geotechnical Research Report No. GEOT-05-06, The University of Western Ontario.

Flügge, W. 1966. “Stresses in shells,” Springler-Verlag, Inc., New York, N.Y.

Hashash, Y. M. A., Hook, J. J., Schmidt, B. and Yao, J. I. 2001. “Seismic design and analysis of underground structures,” Journal of Tunneling and Underground Space Technology, Vol. 16, pp. 247-293.

Hendron, A.J. and Fernandez, G. 1983. “Dynamic and static design considerations for underground chambers,” In: Howard, T.R. (Ed.), Seismic Design of Embankments and Caverns. ASCE, pp. 157–197.

Hindy, A. and Novak, M. 1979. “Earthquake response of underground pipes,” Journal of Earthquake Engineering and Structural Dynamics, Vol. 7, pp. 451-476.

Hindy, A. and Novak, M. 1980. “Earthquake response of buried insulated pipes,” Journal of the Engineering Mechanics Division, ASCE, Vol. 106, No. EM6, pp. 1135-1149.

Jaeger, J. C. and Cook, N. G. W. 1976. “Fundamentals of rock mechanics,” Second Edition, Chapman and Hall, London.

Merritt, J. L., Monsees, J. E. and Hendron, A. J. 1985. “Seismic design of underground structures,” Proc. RETC, Vol. 1.

Morgan, H. D. 1961. “A contribution to the analysis of stress in a circular tunnel,” Geotechnique, London, England, Vol.11, No. 1, pp. 37-46.
Muir Wood, A. M. 1975. “The circular tunnel in elastic ground,” Geotechnique, London, England, Vol.25, No. 1, pp. 115-127.
Peck, R. B., Hendron A J. and Mohraz, B. 1972. “State of the art of soft-ground tunneling,” Proc. RETC, Vol. 1.
Penzien J. and Wu C. L. 1998. “Stresses in linings of bored tunnels,” Journal of Earthquake Engineering and Structural Dynamics, Vol. 27, pp. 283-300.
Penzien J. 2000. “Seismically induced racking of tunnel linings,” Journal of Earthquake Engineering and Structural Dynamics, Vol. 29, pp. 683-691.
Rayhani, M.T., and El Naggar, M.H. 2004. Geotechnical aspects of the Bam earthquake. POLO Earthquake Engineering Workshop, Queen’s University, Canada.
Timoshenko, S. and Goodier, G. N. 1934. “Theory of elasticity,” McGraw-Hill, New York.
Tsang, C. F., Bernier, F. and Davies, C. 2004. “Geohydromechanical processes in the excavation damaged zone in crystalline rock, rock salt, and indurated and plastic clays,” International Journal of Rock Mechanics and Mining Sciences, Vol. 42, pp. 109-125.
Wang, J. N. 1993. “Seismic Design of tunnels,” Monograph 7, Parsons Brinkerhoff Quade & Douglas.
Yuen, C. M. 1979. “Rock-Structure time interaction,” Ph.D. Thesis, The University of Western Ontario, London, Ontario, Canada.